Journal Pre-proofs

Fatigue strength of aluminium welded joints by a non-local approach

Paolo Livieri, Roberto Tovo

PII: S0142-1123(20)30532-6
DOI: https://doi.org/10.1016/j.ijfatigue.2020.106000
Reference: JIJF 106000

To appear in: *International Journal of Fatigue*

Received Date: 29 July 2020
Revised Date: 11 October 2020
Accepted Date: 15 October 2020

Fatigue strength of aluminium welded joints by a non-local approach

Paolo Livieri, Roberto Tovo

Department of Engineering, University of Ferrara, *Via Saragat, 1, 44122 Ferrara,* Italy

Abstract

In this paper, the numerical implicit gradient approach already validated for steel welded joints is also used for aluminium joints. Some peculiarities of aluminium joints are discussed and a general fatigue scatter band for arc welded joints has been proposed. The analysed experimental data taken from the literature range from the simple butt-welded joints with a thickness of 2 mm up to the extruded I-beam with a length of about 2 meters. The obtained SN behaviour has an inverse slope of 3.7 and, at high cycle fatigue, the strength is about half that of steel joints.

Keywords: implicit gradient, fatigue, butt-welded joint, aluminium welded joints

Nomenclature

c	characteristic length, dimensionally a length
k	fatigue curve slope
k_1	non-dimensional coefficient
K_N	notch stress intensity factors (NSIF)
K_f	fatigue strength concentration factors
N	cycles to failure

n	outward normal
P, Q	general points in a continuous domain
Π	scatter index
R	nominal fatigue stress ratio
t	thickness
2α	weld opening angle
Ψ	weight function in non-local stress definition
s	arc length
$\Delta\sigma_{nom}$	reference nominal stress range
σ_{eff}	non-local effective stress (implicit gradient assessment)
$\Delta\sigma_{eff,max}$	maximum range of non-local effective stress
σ_{eq}	equivalent stress
T_{σ}	scatter index

1. Introduction

The design of welded structures not classified in the fatigue design class can only be made by means of local concepts. There are many local methods in the scientific literature that take into account the stress in the neighbourhood of the fillet weld which is thought to be a stress raising factor (for a complete overview see reference [*1*]). In general, the procedure proposed for steel welded joints is also adjusted to aluminium alloy by simply modifying the microstructural parameter or master fatigue curve. Usually, the cycles for nucleation and propagation of a crack up to 1 or 2 millimetres take up most of the life time of the components [*2*, *3*]. This experimental evidence suggests that the local stress or strain field, even without modelling any crack or crack-like defect, can describe the behaviour of the components, under several fatigue loading conditions. Furthermore, another strong simplification can be introduced by setting the notch tip radius equal to zero [*4*]. As recently confirmed by the implicit gradient approach [*5*], if the notch tip radius is very small, for instance significantly less than one millimetre, its actual values and its variation can be neglected, since the geometrical behaviour is comparable to a sharp notch. Conversely, when the notch tip is higher, the fatigue strength increases by increasing the radius and this justifies the advantage given by several post-welding treatments as well as the tig dressing and the grinding [*6*, *7*, *8*]. For this reason, for sharp notches the asymptotic Williams' equations [*9*] results important for the local stress field evaluation in the fatigue life assessments. For example, by integrating Williams' equations, the average strain energy can be evaluated in a circular sector placed at the weld toe; even the Notch Stress Intensity Factors (NSIF) are defined and calculated [*10*, *11*] according to sharp notch stress analysis. With this approach, the fatigue strength of different opening angle can be compared by assessing the most probable zone of crack initiations [*12*]. The NSIF procedure is also a sound theoretical framework for the J-integral approach as proposed in [*13*] where wide mesh can be used for the evaluation of the critical fatigue parameters for both steel and aluminium welded joints. The peach stress method (PSM), proposed in reference [*14*] can also be used the NSIF assessment at the weld with a course mesh [*15*]. Furthermore, the PSM approach is suitable for the fatigue life estimation of both steel and aluminium welded joints by changing the fatigue reference curve [*16*]. A simplified approach to the fatigue calculation is given by the fictitious notch rounding that modify the local geometry by imposing a rounded tip notch [*17*]. However, when the thickness is small the notch tip radius must be changed and the reference fatigue curve have to be changed too accordingly [*1, 18, 19, 20*].

The fatigue assessment of welded structures becomes much more complex when multiaxial loading is involved. The fatigue life of weld can be predicted also with the use of the modified Wohler curve method applied along with the theory of critical distances [*21*]. As highlighted in ref. [*22*], the fatigue damage depends on the whole stress distribution damaging and the material in the vicinity of the crack initiation site uniaxial nominal situations should be treated as simple sub-cases of the more complex multiaxial fatigue problem.

Specifically, the implicit gradient approach provides a weighted averaged stress, where the relevance of the stress is more important at a position closer to the tip. Until now, this method has been suitable for the design of welded joints made of steel, with very different geometry, load conditions and thickness [*23*, *24*, *25*].

The analysis and assessment of fatigue strength in aluminium joints is more difficult due to the reduced availability of experimental data together with the large variability of geometrical features and parent materials. For aluminium alloy, there is generally fewer experimental data present in the scientific literature than that of steel weldments, moreover, many papers do not report detailed data concerning the actual local geometry, such as weld toe angle, throat size and so on. However, in recent years, the role of the so-called *local approaches* has become increasingly more relevant and researchers have paid more attention to local geometry investigation in welded joints.

Furthermore, for aluminium alloys, the ageing condition can modify the mechanical proprieties of the joints and, consequently, this could affect fatigue behaviour even in the welded condition.

This paper focuses on the fatigue strength of fillet and butt welded joints, where the geometrical effect is assumed to be predominant. Hence, as a first approximation, the same characteristic strength is applied to all types of aluminium alloys, similarly to steel welded joints, as already applied in several design standards for the aluminium alloys [*26*, *27*]. As a first approach, the local changes in mechanical properties due to the welding process are not considered either, or are they considered in any other local, structural or nominal stress approach to fatigue design of welded joints. However, this assumption is suitable particularly when geometrical the stress raising effect is dominant. Otherwise, for instance in friction stir welding, when the geometrical notch effect is reduced, the ageing beneficial is no longer negligible and a separate investigation among different aluminium alloys is more appropriate [*28, 29*].

The aim of this paper is to investigate the fatigue strength of aluminium welded joints taken from the literature. The implicit gradient approach is used to estimate the fatigue main curve of aluminium alloy by considering different geometrical shapes. Many experimental data divided into test series have been investigated and a different characteristic length relating to the material proprieties has been proposed for aluminium joints.

2 The non-local implicit gradient approach

The fatigue damage at stress concentrations could be related to an average value of stress as originally suggested by Neuber [*30*]. Over the last decade, the idea has been successively revisited in several papers and contributions, see for instance refs. [*31*, *32, 33*]. The Neuber idea can be generalised at any point of the structural component by means of a weight function that considers the nearest points and its stress fields more critical [*34*, *35*, *36*].

Actually, the equivalent stress obtained by means of the implicit gradient method applies the calculation of the average stress at the stress raiser [*37*, *38*]. Usually in welded joints, the cracks nucleate at the weld toe or root due to fatigue loading. This aspect is checked in all experimental papers that experimentally analyse the nucleation and the propagation of the crack by means of failure analysis after the final collapse [*39*]. However, there are a few exceptions that are related to the presence of defects in the weld [*40*] or, in the case of spot welds, that are due to a relevant of shear loading [*24, 41*].

By accepting the simplification that the weld can be idealised as a Sharp V-notch, the local stress field can be mathematically described by means of Williams' asymptotic equations.

Such an elastic stress field is considered here in the analytical form proposed in ref. [*42*]:

$$\begin{Bmatrix} \sigma_{\vartheta\vartheta} \\ \sigma_{rr} \\ \tau_{r\vartheta} \end{Bmatrix} = \frac{1}{\sqrt{2\pi}} \frac{r^{\lambda_1 - 1} K_{N,1}}{(1+\lambda_1)+\chi_1(1-\lambda_1)} \cdot \begin{Bmatrix} f_{\vartheta,1}(\vartheta) \\ f_{r,1}(\vartheta) \\ f_{r\vartheta,1}(\vartheta) \end{Bmatrix} \qquad (1)$$

for mode I, and

$$\begin{Bmatrix} \sigma_{\vartheta\vartheta} \\ \sigma_{rr} \\ \tau_{r\vartheta} \end{Bmatrix} = \frac{1}{\sqrt{2\pi}} \frac{r^{\lambda_2 - 1} K_{N,2}}{(1-\lambda_2) + \chi_2 (1+\lambda_2)} \cdot \begin{Bmatrix} f_{\vartheta,2}(\vartheta) \\ f_{r,2}(\vartheta) \\ f_{r\vartheta,2}(\vartheta) \end{Bmatrix} \quad (2)$$

for mode II, where χ_i and μ_i are geometric parameters, λ_i Williams' eigenvalues, $f_{i,j}$ harmonic functions and $K_{N,i}$ are calculated by applying the definition proposed by Gross and Mendelson [*43*]. For a generic welded joint characterised by an opening angle 2α, Notch Stress Intensity Factors (NSIFs) can be obtained from an accurate asymptotic FE analysis [*44*]:

If the opening angle is larger than 102°, only mode I is singular and if the $K_{N,1}$ is known, the effective stress, $\sigma_{eff,}$ relates to the average stress fields generated by a stress raiser and, as well as a sharp V-notch, it can be analytically estimated by using the implicit gradient method as [*45*]:

$$\sigma_{eff,max} = \frac{m_v}{c^{1-\lambda_1}} K_{N,1} \quad (3)$$

where m_v is a non-dimensional parameter that depends only on the opening angle and λ_1 is Williams' eigenvalue of mode I (for 2a=0 and 135°, λ_1 assumes values of 0.5 and 0.674, respectively). The parameter m_v is equal to 0.405 for 2α equal to 135° [*45*], and *c* is the characteristic length.

In a more general case, the NSIFs are not known, so the effective stress σ_{eff} can be calculated numerically, point by point, by solving the Helmholtz differential equation in volume V of the component by imposing Neumann boundary conditions [*46*]:

$$\sigma_{eff} - c^2 \nabla^2 \sigma_{eff} = \sigma_{eq} \quad \text{in} \quad V \quad (4)$$

In Eq. (4) it is assumed that fatigue damage is related to the average value of a physical quantity evaluated on the whole component. It is usually related to the multiaxial adopted criterion and is called equivalent stress σ_{eq}. ∇^2 is the Laplace operator. Neuman boundary conditions are assumed: $\nabla\sigma_{eff} \cdot n = 0$ (where $\nabla\sigma_{eff}$ is the gradient of the effective stress and *n* is the outward normal to the boundary). *c* is the characteristic length assumed constant and related only to the material, in this case an aluminium alloy in as welded condition. The value of effective stress σ_{eff} closely depends on the value of *c*. When *c* is small, the effective stress σ_{eff}(P) approaches σ_{eq} (P), while when *c* increases, the effective stress becomes less sensible to the stress concentration. For this reason, it is important to correctly evaluate *c* for a given material. The value of *c* can be evaluated on the basis of experimental result at high cycle fatigue. In the case of sharp V-notches, from Equation (3), by imposing that the effective stress will be constant independently of the opening angle, it is possible to evaluate *c*. In this case it is necessary to have at least two series of experimental data relative to two different opening angles. In the case of welded joints, a detailed discussion is given in section 4.

Equation (4) can be solved by means of FE analysis, even by using the same mesh utilised for the previous calculation of σ_{eq} related to the Cauchy stress tensor under linear elastic hypothesis of the material. A non-linear behaviour could be introduced without particular problems as well as a multiaxial fatigue criterion [*47*, *48*, *49*]. Although the equivalent stress can be singular at the notch tip, the effective stress results in a continuous function and this strongly simplifies the fatigue assessments of welded structures, and in general, sharp V-notches.

With the implicit gradient approach, by solving Eq. (4) we indirectly evaluate, in a convenient numerical form, the average stress σ_{av} in each point of the weld. The definition of the average stress linked to the σ_{eff} is given by [*46*]:

$$\sigma_{av}(P) = \frac{\int_V Y(P,Q)\, \sigma_{eq}(Q)\, dV}{\int_V Y(P,Q)\, dV} \tag{5}$$

where: P is the investigated point; Q a generic variable point inside volume V of the Ω body and the equivalent stress σ_{eq} a function of the stress tensor. The weight function Ψ is an isotropic function of the distance *s*, which vanishes as the distance between P and Q increases. Figure 1, proposes the concept of the implicit gradient approach.

Now, by recalling the linear proportionality between the NSIF $K_{N,1}$ and the nominal stress σ_{nom} ($K_N = k_1\, t^{1-\lambda_1}\, \sigma_{nom}$; where k_1 is a non-dimensional coefficient, σ_{nom} the range of the remote applied stress and *t* the main plate thickness of the joints [*4*]), the fatigue strength concentration factor K_f can be defined in the form

$$\sigma_{eff,max} = \frac{m_v\, k_1\, t^{1-\lambda_1}}{c^{1-\lambda_1}} \cdot \sigma_{nom} = K_f \cdot \sigma_{nom} \tag{6}$$

Note that K_f takes into account both geometrical effect and material sensitivity in a unique non-dimensional parameter as is usual for the fatigue notch strength reduction factor. Obviously, under fatigue loading the Eq. (6) can be written in terms of stress range:

$$\Delta\sigma_{eff,max} = \frac{m_v\ k_1 t^{1-\lambda_1}}{c^{1-\lambda_1}} \cdot \Delta\sigma_{nom} = K_f \cdot \Delta\sigma_{nom} \tag{7}$$

Equation (6) can also be used when the NSIF is not available. In this case the effective stress can be evaluated by means of Eq. (4) for a given value of *c* and applied nominal stress $\cdot\, \sigma_{nom}$. Then, after the numerical calculus of $\sigma_{eff,max}$, by assuming that mode I is dominant, k_1 can be calculated.

As an example, Figure 2 shows the effective stress for rectangular hollow section joints when a remote axial loading σ_{nom} is applied to the chord (AL-27 series [*50*]). The coloured scale indicates the most critical point without any further post processing of the data. Furthermore, in order to quantify the effective stress, a plot of effective stress along the weld toe is suggested. Figure 2 reports the effective stress in dimensionless form along the path ABCD as a function of arc length *s* for a *c* value of 0.15 mm. The maximum value is reached near point *C* (nominal opening angle 2α=125°). From Eq. (6), k_1 results as 1.53 with thickness *t* being equal to 3 mm.

3 The implicit gradient approach in fatigue welded joint assessment

The effective stress at the weld tip can be easily evaluated by means of Eq. (3) if the NSIF of mode I is known. On the other hand, for complex geometries, the implicit gradient approach can take advantage of any user-defined partial differential equation solver, for instance the FE numerical procedure implemented in Comsol Multiphysics FE software. For welded structures subjected mainly to a mode I loading, a reasonable option is to assume σ_{eq} equal to the maximum principal stress σ_1, which is evaluated with a conventional finite element investigation for linear elastic materials [*51*]. The Helmholtz Eq. (4), is solved by using the same mesh required for the previous FE analysis where the Cauchy stress tensor is calculated. The mesh refinement does not require any special rules: the analytical problem only has one finite solution and a simple numerical convergence analysis is suitable. Generally, near the critical point, an element size close to the size of characteristic length *c* is appropriate. An example of an accurate convergence analysis applied to the implicit gradient application is available in reference [*24*]. The equivalent stress is calculated all over the geometry; but, in general, its maximum value is usually at the weld toes or at the weld roots. The location of the maximum effective value of the equivalent stress defines the critical point.

In comparison with the other local approaches listed in the introduction and presented, for instance, in reference [1], our method offers some interesting peculiarities such as:

- it is independent of the shape of the joints, load type and main plate thickness;

- it is suitable for both two-dimensional or three-dimensional models by referring to the same SN curve;

- it does not require any modification of the geometry or CAD three-dimensional model and any geometrical detail can be considered, including real or assumed defects;

- the crack initiation site is not assumed a priori, but it results from the analysis and, in previous investigations, it agrees with the experimental evidence;

- it does not require any structured or particular rule for FE mesh creation;

- under multiaxial loading it is possible to implement a consistent procedure that takes into account the effects of multiaxiality.

On the contrary, a disadvantage is that the method requires the use of multi-physics software that is able to solve the Helmholtz partial differential equation of second order. Hence two FE analyses are necessary: the first is a conventional FE structural analysis to evaluate the Cauchy tensor and the second to solve Equation (4). If useful, the two FE analyses can use the same mesh.

3.1 Steel joints

In previous papers, the authors considered the fatigue strength of welded joints made of steel. More than one thousand experimental data from past works were considered and the behaviour of welded joints can be summarised by means of a universal scatter band in terms of maximum range of effective stress $\Delta\sigma_{eff, max}$. In the case of arc welded joints made of steel, the fatigue scatter band was evaluated between 10^4 and $5 \cdot 10^6$ cycles to failure. The inverse slope turned out to be close to 3 and the T_σ ratio between the scatter bands related to the mean values plus/minus 2 standard deviations was 1.9. The scatter band is independent from the geometry of the joints and can be used to estimate the safety factor of welded joints or to estimate fatigue life in terms of nominal stress [*51, 5*].

Figure 3 shows the capability of $\Delta\sigma_{eff, max}$. to recap the fatigue strength of about 600 experimental points of welded joints of very different geometries and main plate thicknesses (from 3 up to 100 mm). The design curve for automatic heat cutting FAT 140 proposed by Eurocode [*52*] is very close to the curve of 97.7% survival given by the implicit gradient approach so that the reference curve of the effective stress is actually the already assessed design strength of the parent material affected by a thermal process.

3.2 Aluminium welded joints

This section analyses the fatigue behaviour of welded joints made of aluminium alloy by using the design procedure tuning for steel joints. The experimental data taken from the literature can be divided into four groups. The first set is reported in Table 1. The welded joints in Table 1 were previously analysed and qualified by the NSIF of mode I. The opening angle ranges from 135° to 180°. The FE analysis used for the NSIF assessments was of the two-dimensional type (for further details see reference [*12*]).

The second, third and the fourth sets of experimental data are newly analysed data and the effective stress is numerically evaluated by proper numerical integrations of Eq. (4). For these welds, the numerical analyses are based on three-dimensional models so that the local effect due to the relationship between the thickness and the transversal size of the weld can be fully considered, as underlined in reference [*25*]. Table 2 reports the main characteristic of T-welded joints, butt-welds, butt-welds with incomplete penetration, and hollow T-joint sections subjected to axial or bending loadings characterised by a sharp V-notch. Table 3 and 4 summarise other series of fatigue data that will be used for the confirmation of the scatter band defined by using experimental data from Tables 1 and 2.

The three-dimensional models analysed in Tables 2–4 respect the geometrical size reported in the original papers. However, in order to define an accurate virtual model, some dimensions are taken from pictures presents in the same papers.

First of all, Fig. 4 suggests the analysis of all data in terms of nominal stress. Tables 1–4 report the value of fatigue strength of nominal stress at 5×10^6 cycles to failure and 50% probability of survival. The scatter is very high and a rational single synthesis by means of a simple use of the nominal stress is not possible.

In order to calculate the effective stress, the definition of the characteristic length *c* is of fundamental importance. The *c* value can be evaluated in different ways; but, due to the scatter of the fatigue behaviour, differences can arise by changing assessment procedure.

For instance, a first possibility is to compute "*c*" by fitting different reference high cycle fatigue strength values, usually at 5×10^6 cycles to failure for 50% probability of survival. It is possible to consider the fatigue strength of welded joints with an opening angle 2α =135° and the ground butt welds (2α=180°), from data reported in Table 5. By comparing the effective stress from Eq. (3) to the fatigue limit, *c* results as:

$$c = \left(\frac{m_v \cdot \Delta K_N}{\Delta\sigma_{nom}}\right)^{\frac{1}{1-\lambda_1}} \tag{8}$$

and from data from Table 5*, c* turns out to be close to 0.09 mm.

Another possibility is to use all experimental data available in the range of 10^4 to 10^7 of cycles to failure.

For the welded joints of Table 1, σ_{eff} was evaluated by means of Eq. (3), while for the welds of Table 2, a numerical three-dimensional solution was considered and K_1 was evaluated for each series. Then, under the hypothesis of dominant mode I loading, the $\Delta\sigma_{eff,max}$ can be written in the former case indicated by Eq. (7) as a function of the *c* values.

Concerning fatigue life assessment, the analytical model for predicting fatigue life is the classic linear model in a double logarithm scale (Wohler curve: ${\Delta\sigma_{eff,max}}^k \cdot N = constant$). If we consider the welded joints in Tables 1 and 2, for a given value of *c*, the scatter index Π can be evaluated in the form

$$\Pi = \sum d^2 \tag{9}$$

where d is the difference between the logarithm of experimental cycles to fatigue and the logarithm of the analytic model.

By so doing, the scatter index Π divided by its minimum value Π_{min} can be expressed numerically as a function of c. Figure 5, shows that the minimum of Π is close to 0.15 mm.

Figure 6, reports the $\Delta\sigma_{eff,max}$ against cycle to fatigue. A scatter band can be defined in a similar way as welded joints made of steel. The slope is different, 3.7 versus 3.0, and the scatter index T_σ increases up to 2.3.

In order to confirm the scatter band of Figure 6, the analysis was completed with joints from Tables 3 and 4. In many series in Table 3, the weld toe is rounded. The implicit gradient approach is also suitable in these cases because the numerical procedure supports the actual geometry and also a three-dimensional model from a 3D digitising real-world object can be used [*23*]. The welded joints in Tables 4 are more complex and the size is greater than the previous one. The beams were subjected to bending loading. The extruded profiles, I or T beams, were welded to transversal stiffeners or the plates were welded to the flange profile under positive tensile loading. In this paper, for the sake of simplicity, the four-point bending, for series 39–41 and 43, was simulated by means of a couple of force applied at the end of the beam. Then, the K_f was evaluated for all the series, which is reported in Tables 1–4.

Figure 7 summarises about 600 experimental points analysed in this paper. Specimens with different geometries and thicknesses ranging from 2 to 25 mm present similar fatigue strength in terms of effective stress.

Finally, Figure 8 and Table 6 resume the two universal scatter bands for welded structures made of steel or aluminium alloy. The adopted numerical procedure is always the same regardless of geometry, size and material. The difference in steel or aluminium alloy is only due to the material c parameter.

.

4 Conclusions

The main conclusions of this paper can be summarised as follows:

- For aluminium welded joints, many experimental data sets are available in the literature, however, only a small number has actually been considered since the power of a three-dimensional approach is only possible when a sound picture or sketch of the actual weld geometry is given.
- A scatter band was obtained in terms of the effective stress range by analysing aluminium welded joints with the main plate thickness ranging from 2 to 25 mm.
- The scatter band allows the designer to predict the fatigue life of aluminium welded joints without changing the procedure with respect to the algorithm proposed for welded joints made of steel. The characteristic length for aluminium alloy reduces to 0.15 mm (0.2 mm for steel joints). However, in relation to the steel joints, the scatter index increases by about 20%.
- The soundness of the implicit gradient approach to aluminium welded joints was verified based on the three-dimensional numerical procedure of about 600 experimental points.
- The proposed approach is suitable for fatigue life assessment of welded joints characterised by different opening angles of the fillet, different sharpness of the weld toe and different thicknesses.
- To reduce the scatter of the fatigue curve, the actual weld geometry must be known. In fact, with a three-dimensional numerical procedure such as the implicit gradient approach, it is possible to consider the influence of any weld geometry detail.

Figure 1. implicit gradient reference geometry

Fig. 2. Effective stress in dimensionless form for the rectangular hollow section joints under axial loading σ_{nom} (chord) of AL-27 series. s is the arc length along the weld toe with the origin at point A belonging to the longitudinal symmetry axis (c=0.15 mm)

Fig. 3. Scatter band of steel welded joints of about 600 experimental points in terms of maximum effective stress range (scatter bands related to mean values plus/minus 2 standard deviations; NLC: non-load-carrying joint, LC: load-carrying joint)

Fig. 4. Scatter band for aluminium welded joints in terms of maximum nominal stress range (scatter bands related to mean values plus/minus 2 standard deviations)

Fig. 5. Scatter index as a function of the *c* characteristic length

Fig. 6. Scatter band for aluminium welded joints in terms of maximum effective stress range (scatter bands related to mean values plus/minus 2 standard deviations)

Fig. 7. Scatter band for aluminium welded joints in terms of maximum effective stress range (scatter bands related to mean values plus/minus 2 standard deviations)

Fig. 8. Scatter bands for steel and aluminium welded joints in terms of maximum effective stress range (scatter bands related to mean values plus/minus 2 standard deviations)

Table 1. Geometrical and fatigue strength properties of aluminium welded joints (two-dimensional analysis, for details see reference [*12*])

Series	Refs	Material	t [mm]	R	$\Delta\sigma_{n,50\%}$	$\Delta K^{N}_{1,\,50\%}$ $5 \cdot 10^6$ cicli	$\sigma_{eff,50\%}$ $5 \cdot 10^6$ cicli	K_f

						$5 \cdot 10^6$ cicli [MPa]	MPa $mm^{0.326}$	MPa	C=0.15 mm
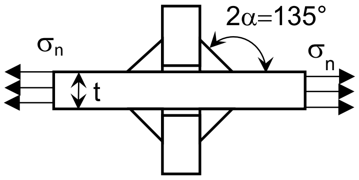	AL-1	Maddox [53]	6061-T6	3	0.1	59.3	103.2	77.6	1.31
	AL-2	Maddox [53]	6061-T6	6	0.1	45.3	97.8	73.5	1.62
	AL-3	Maddox [53]	6061-T6	12	0.1	40.5	108.6	81.6	2.02
	AL-4	Maddox [53]	6061-T6	24	0.1	29.1	97.7	73.4	2.52
	AL-5	Maddox [53]	6061-T6	24	0.1	40.9	105.0	78.9	1.93
C-NLC	AL-6	Maddox [53]	6061-T6	12	0.1	38.0	94.1	70.7	1.86
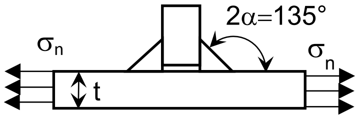	AL-7	Meneghetti [54]	5083-H3	12	0.1	43.1	89.7	67.4	1.56
T-NLC	AL-8	Ribeiro [55]	6061-T651	12	0.1	53.0	110.3	82.9	1.56
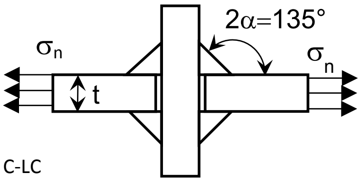	AL-9	Ribeiro [55]	6061-T651	12	0.1	28.0	108.8	81.8	2.92
C-LC	AL-10	Jacoby [56]	Al Zn Mg 1	12	0.1	27.4	127.5	95.9	3.50
	AL-14	Ohno [57]	5083-O	4	0	86	-	86	1
	AL-15	Person [58]	5052-H32	4.8	0	92	-	92	1
	AL-16	Person [58]	5083-H113	9.5	0	100	-	100	1
	AL-17	Person [58]	5083-H113 : 6061-T6	9.5	0	100	-	100	1
G-BW	AL-18	Person [58]	5086-H32	9.5	0	107	-	107	1
	AL-19	Person [58]	7039-T61	9.5	0	102	-	102	1

Key:

Type of joint: C-NLC = cruciform joint with non-load carrying fillet weld; C-LC = cruciform joint with load-carrying fillet weld; T-NLC =T-joint with non-load carrying fillet weld; G-BW = ground butt weld

Table 2. Geometrical and fatigue strength properties of aluminium welded joints (sharp V-notch)

Refs	Series	3D model	Type of joint Type of loading Opening angle Material Load ratio	t [mm]	$\Delta\sigma_{n,50\%}$ $5 \cdot 10^6$ cicli [MPa]	K_f C=0.15 mm
Sidhom et al. [*59*]	AL-20	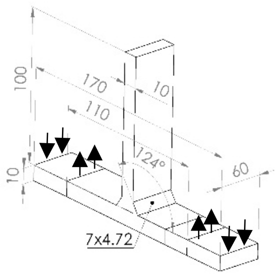	T-joint Four-point bending 124° 5083 H11 0.1	10	42.0	2.15
Morgenstern et al. [*60*]	AL-21	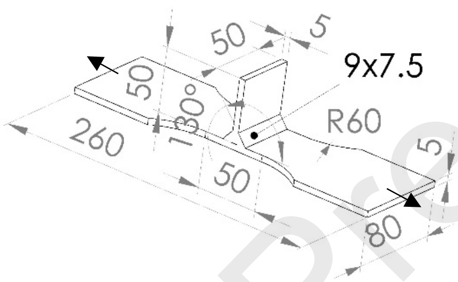	T-joint Tensile loading 130° AW-6082 T6 0	5	73.7	1.34
Haagensen et al. [*61*]	AL-22	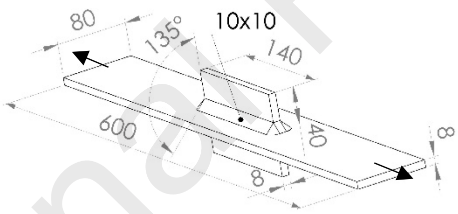	Longitudinal stiffeners Tensile loading 135° AA 5083 0.1	8	28.7	2.75
Haagensen et al. [61]	AL-23	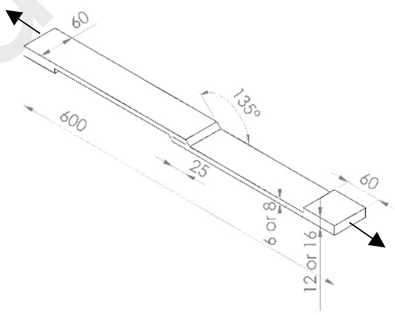	Lap joint Tensile loading 135° AA 5083 0.1	6	16.3	5.90

Haagensen et al. [61]	AL-24	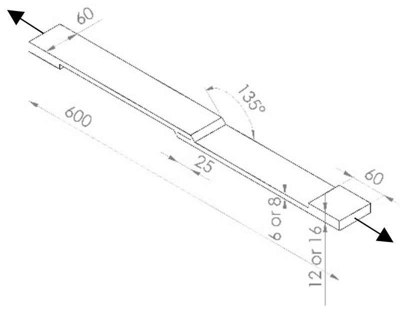	Lap joint Tensile loading 135° AA 5083 0.1	8	10.8	6.41
Brandt et al. [*62*]	AL-25	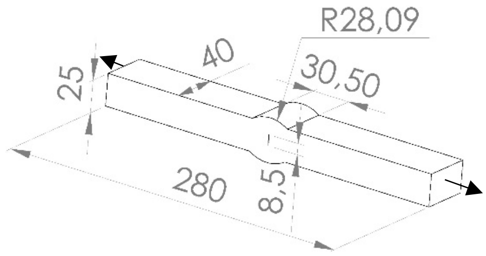	Butt joint with incomplete penetration Tensile loading 0° AA 5083 Stress-relief annealed 0	25	21.7	6.41
Macdonald et al. [*63*]	AL-26	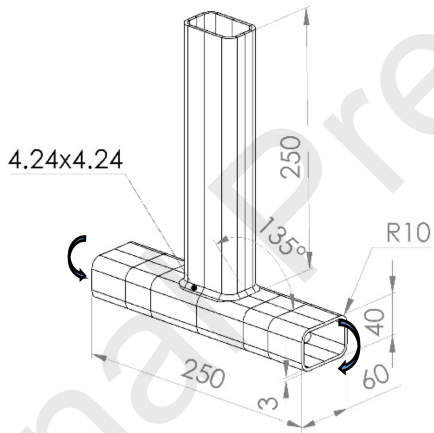	Rectangular hollow section joints Pure bending of the chord member 135° 6082.26-T5 0.1	3	31.6	2.36
Macdonald et al. [50]	AL-27	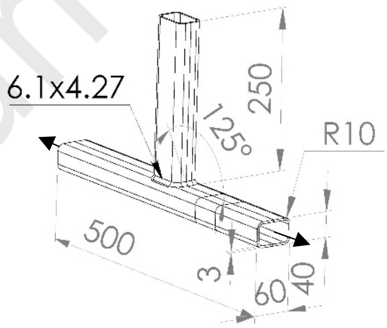	Rectangular hollow section joints Axial loading, chord 125° 6060.35-T5 0.1	3	35.4	2.06

Macdonald et al. [50]	AL-28	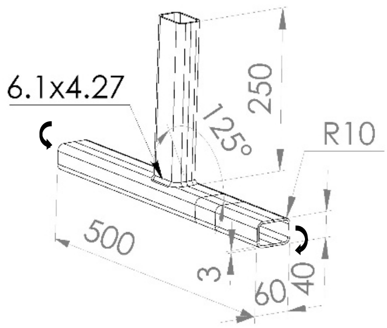	Rectangular hollow section joints Four-point bending chord 125° 6060.35-T5 0.1	3	38.5	2.51
Macdonald et al. [50]	AL-29	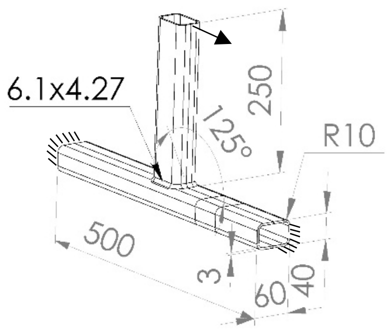	Rectangular hollow section joints In-plane bending branch 125° 6060.35-T5 0.1	3	13.8	8.80

Table 3. Geometrical and fatigue strength properties of aluminium welded joints (others series)

Refs	Series (partition)	3D model	Type of joint, Type of loading Opening angle Material Load ratio	Thickness of main plate [mm]	$\Delta\sigma_{n,50\%}$ $5 \cdot 10^6$ cicli [MPa]	K_f C=0.15 mm
Brandt et al. [62]	AL-30 (1/8)	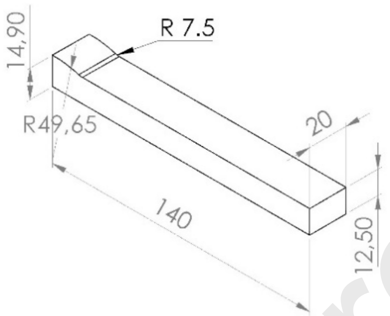	Butt weld Axial loading 162° AA5083 (stress-relief annealed) 0	25	54.2	1.38
Brandt et al. [62]	AL-31 (1/8)	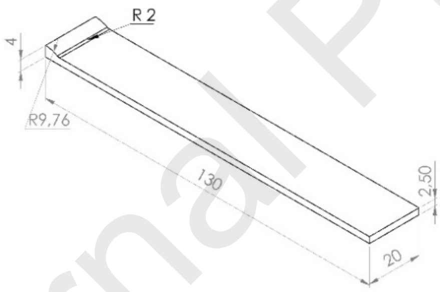	Butt weld Axial loading 148° AA5083 (stress-relief annealed) 0	5	43.2	1.36
McDowell [*64*]	AL-32 (1/8)	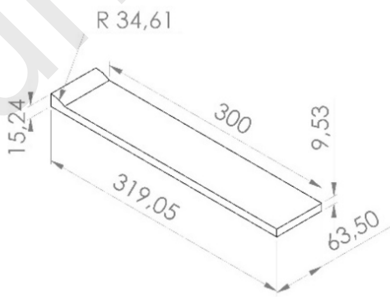	Butt weld Axial loading 147° 5456-H117 ~0	19.05	48.7	2.11

McDowell [64]	AL-33 (1/8)	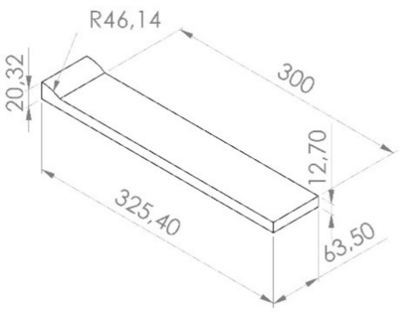	Butt weld Axial loading 147° 5456-H117 ~0	25.4	71.5	2.26
Shahani et al. [*65*]	AL-34 (1/8)	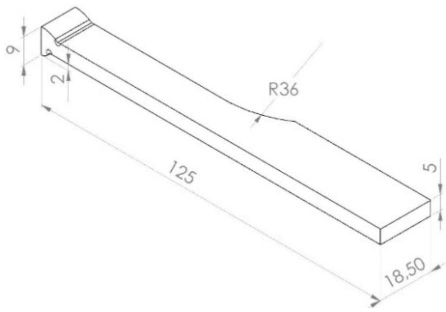	Butt weld Axial loading 110° Al5456-H38 0.01	5	39.5	1.77
Shahani et al. [65]	AL-35 (1/8)	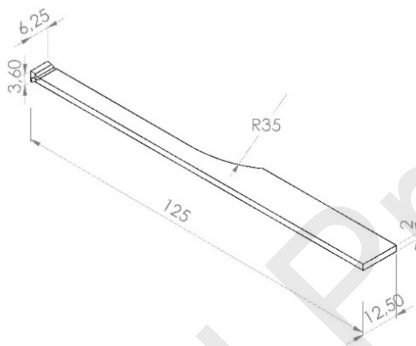	Butt weld Axial loading 110° Al5456-H38 0.01	2	59.8	1.30
Viespoli et al. [*66*]	AL-36 (1/8)	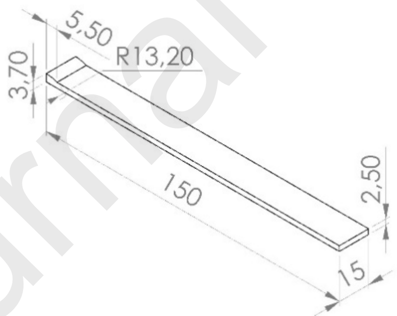	Butt weld Axial loading 148° AA6082 - T6 0	5	65	1.39
Viespoli et al. [66]	AL-37 (1/8)	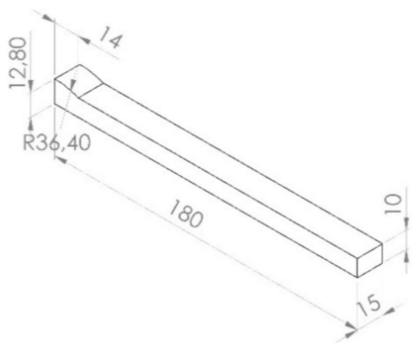	Butt weld Axial loading 148° AA6082 - T6 0	20	47.6	1.70

Coughlin et al. [67]	AL-38 (1/8)	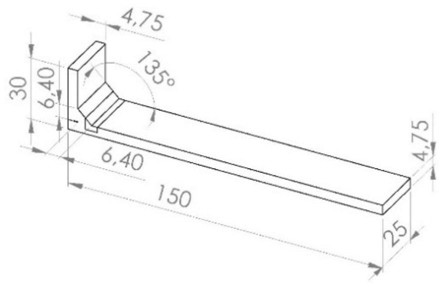	non-load carrying cruciform joint Axial loading 135° 6061-T651 0.1	9.5	47.7	2.07

Table 4. Geometrical properties of aluminium welded joints (extruded beams)

Refs	Series	3D model	Type of joint Type of loading Opening angle Material Load ratio	Thickness of main plate [mm]	$\Delta\sigma_{n,50\%}$ $5 \cdot 10^6$ cicli [MPa]	K_f C=0.15 mm
James et al. [*68*]	AL-39	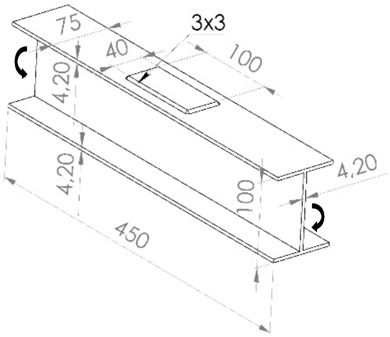	Extruded I-beams Four-point bending 135° 6261-T6 0.1	4.2	35.0	2.81
James et al. [68]	AL-40	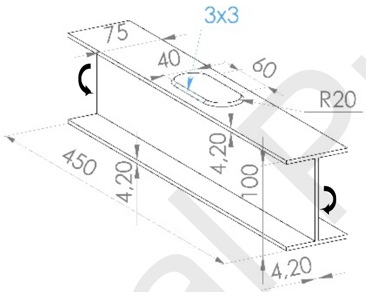	Extruded I-beams Four-point bending 135° 6261-T6 0.1	4.2	37.5	2.98
James et al. [68]	AL-41	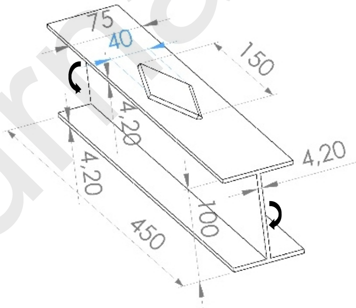	Extruded I-beams Four-point bending 135° 6261-T6 0.1	4.2	37.6	2.70
Tveiten et al. [*69*]	AL-42	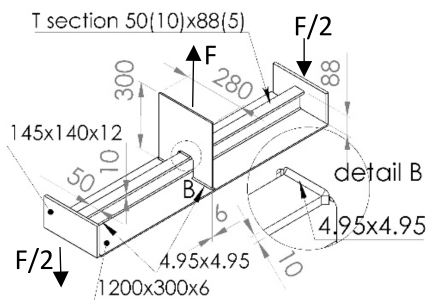	Extruded T-beams Three-point bending 135° 6082-T6 0.1	10	26.6	3.82

Hirt et al. [70]	AL-43	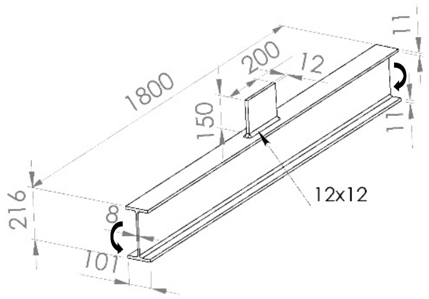	Extruded I-beams Four-point bending 135° 6082 (Anticorodal 112-T6) 0.1	11	23.1	4.32

Table 5. Notch Stress Intensity Factors and nominal stress range related to a 50% probability of survival at $N=5\cdot10^6$ cycles, for a nominal load ratio $R \approx 0$ in as-welded state (for details see Ref. [*12*])

2α	steel		aluminium alloy	
	0°	135°	135°	180°
	$\Delta K_{N,1}$ = 180 MPa $mm^{0.5}$	$\Delta K_{N,1}$ = 211 MPa $mm^{0.326}$	$\Delta K_{N,1}$ = 99 MPa $mm^{0.326}$	$\Delta\sigma_{nom}$ = 96 MPa

Table 6. Reference value of the effective stress of the two fatigue scatter bands at $5 \cdot 10^6$ cycles to failure

Weld type	97.70% [MPa]	50% [MPa]	2.30% [MPa]	k
steel	111	156	219	3.0
aluminium	53.4	80.1	121	3.7

References

1 Radaj D, Sonsino CM, Fricke W. Fatigue assessment of welded joints by local approaches. 2nd ed. Cambridge: Woodhead Publishing; 2006

2 Lassen, T. The effect of the welding process on the fatigue crack growth. Welding Journal 1990; **69**, Research Supplement, 75S–81S

3 Mikulski Z, Lassen T. Fatigue crack initiation and subsequent crack growth in fillet welded steel joints. International Journal of Fatigue 2019; 120: 303–318

4 Lazzarin P, Tovo R, 1998. A Notch Intensity Approach to the Stress Analysis of Welds. Fatigue and Fracture of Engineering Materials and Structures 21, pp. 1089–1104

5 Livieri P, Tovo R. Overview of the geometrical influence on the fatigue strength of steel butt welds by a non-local approach. *Fatigue Fract Eng Mater Struct*. 2019; 1–12. https://doi.org/10.1111/ffe.13135

6 Marquis, GB, Barsoum, Z. IIW Recommendations on High Frequency Mechanical Impact (HFMI) Treatment for Improving the Fatigue Strength of Welded Joints Springer IIW Collection 2016

7 Zhang YH, Maddox SJ. Fatigue life prediction for toe ground welded joints, International Journal of Fatigue 31 (2009) 1124–1136

8 Haagensen J, Maddox SJ. IIW recommendations on methods for improving the fatigue strength of welded joints_ IIW-2142-110-Woodhead Publish

9 Williams ML. Stress singularities resulting from various boundary conditions in angular corner of plates in extension. ASME Journal of applied Mechanics 1952; 19: 526–528

10 Lazzarin P, Zambardi R. A finite-volume-energy based approach to predict the static and fatigue behaviour of components with sharp V-shaped notches. International Journal of Fracture 2001; 112: 275–298.

11 Berto F, Lazzarin P. A review of the volume-based strain energy density approach applied to V-notches and welded structures, Theoretical and Applied Fracture Mechanics 52 (2009) 183–194

12 Livieri P, Lazzarin P, 2005. Fatigue strength of steel and aluminium welded joints based on generalised stress intensity factors and local strain energy values, International Journal of Fracture, 133, pp. 247–376

13 Livieri P, Tovo R. The use of the J_V parameter in welded joints: stress analysis and fatigue assessment. International Journal of Fatigue 2009; 31(1): 153–163

14 Meneghetti G, 2008. The Peak Stress Method Applied To Fatigue Assessments Of Steel And Aluminium Fillet-Welded Joints Subjected To Mode I Loading Fatigue & Fracture Of Engineering Materials & Structures 31–5, pp: 346–369

15 Campagnolo A, Meneghetti G, Berto F. Rapid finite element evaluation of the averaged strain energy density of mixed-mode (I + II) crack tip fields including the T-stress contribution, Fatigue and Fracture of Engineering Materials and Structures 39(8), 2016, 982–998

16 Meneghetti G, Campagnolo A, Rigon D. Multiaxial fatigue strength assessment of welded joints using the Peak Stress Method – Part I: Approach and application to aluminium joints. International Journal of Fatigue 101 (2017) 328–342

17 Radaj D. *Design and analysis of fatigue resistant welded structures* 1990, Abington Publishing, Abington, Cambridge.

18 Hobbacher A. Recommendations for fatigue design of welded joints and components. Paris, IIW: International Institute of Welding; 2007. Document XIII-1823e07/XV-1254-07

19 Karakas Ö, Morgenstern C, Sonsino CM, 2008. Fatigue design of welded joints from the wrought magnesium alloy AZ31 by the local stress concept with the fictitious notch radii of rf=1.0 and 0.05 mm, International Journal of Fatigue, 30–12, pp. 2210–2219. International Journal of Fatigue, Vol. 101–2, pp. 363–370

20 Marulo G, Baumgartner J, Frendo F, 2017. Fatigue strength assessment of laser welded thin-walled joints made of mild and high strength steel, International Journal of Fatigue 96, pp. 142–151

21 Susmel L, Taylor D, 2011. The Theory of Critical Distances to estimate lifetime of notched components subjected to variable amplitude uniaxial fatigue loading, International Journal of Fatigue, Vol. 33, 7, pp. 900–911

22 Susmel L, Modified Wohler curve method, theory of critical distances and Eurocode 3: A novel engineering procedure to predict the lifetime of steel welded joints subjected to both uniaxial and multiaxial fatigue loading, International Journal of Fatigue 30 (2008) 888–907

23 Livieri P, Tovo R. The effect of throat underflushing on the fatigue strength of fillet weldments. Fatigue & Fracture of Engineering Materials & Structures 2013; 36(9): 884–892

24 Tovo R, Livieri P, 2011. A numerical approach to fatigue assessment of spot weld joints. Fatigue and Fracture of Engineering Materials and Structures, Vol. 34-1, pp. 32–45

25 Livieri P, Tovo R. Analysis of the thickness effect in thin steel welded structures under uniaxial fatigue loading. International Journal of Fatigue 2017; 101 (Part 2): 363–370, DOI: 10.1016/j.ijfatigue.2017.02.011

26 EN 1999-1-3:2007 Eurocode 9: Design of aluminium structures – Part 1–3: Structures susceptible to fatigue

27 Hobbacher, AF, 2016. Recommendations for fatigue design of welded joints and components. Second edition, IIW document IIW-2259-15

28 Lomolino S, Dos Santos J, Tovo, R. On the fatigue behaviour and design curves of friction stir butt-welded Al alloys, Int. J. Fatigue, Vol. 27, N. 3, pp. 305–316, 2005

29 Maggiolini, E, Benasciutti, D, Susmel, L, Hattingh, DG, James, MN, Tovo, R. Friction stir welds in aluminium: Design S-N curves from statistical analysis of literature data (2018) Fatigue and Fracture of Engineering Materials and Structures, 41 (11), pp. 2212–2230. DOI: 10.1111/ffe.12805

30 Neuber H. Kerbspannungslehre. Springer 1957 Berlin

31 Atzori B, Lazzarin P, Tovo R. Stress field parameters to predict the fatigue strength of notched components. J Strain Anal Eng. 1999; 34 (6): 437–453

32 Susmel L, Taylor D. The Theory of Critical Distances to estimate the static strength of notched samples of Al6082 loaded in combined tension and torsion. Part I: Material cracking behaviour, Engineering Fracture Mechanics 77 (2010) 452–469

33 Taylor D. Geometric effects in fatigue: a unifying theoretical model. International Journal of Fatigue, 1999, **21**: 413–420

34 Eringen CA. Nonlocal polar elastic continua. International Journal of Engineering Science, 1972, 10: 1–16

35 Pijaudier-Cabot G, Bažant ZP, 1987. Nonlocal Damage Theory, Journal of Engineering Mechanics, 10, pp. 1512–1533

36 Weixing, Y, 1993. Stress field intensity approach for predicting fatigue life. International Journal of Fatigue 15, pp. 243–245

37 Peerlings RHJ, Geers MGD, de Borst R, Brekelmans WAM. A critical comparison of nonlocal and gradient-enhanced softening continua. International Journal of Solids and Structures, 2001, **38**: 7723–7746.

38 Maggiolini E, Livieri P, Tovo R, 2015. Implicit gradient and integral average effective stresses: Relationships and numerical approximations, Fatigue & Fracture of Engineering Materials & Structures, Vol. 38–2, pp. 190–19

39 Maddox SJ. Review of fatigue assessment procedures for welded aluminium structures, International Journal of Fatigue 25 (2003) 1359–1378

40 Livieri P, Tovo R. The effect of throat underflushing on the fatigue strength of fillet weldments. Fatigue & Fracture of Engineering Materials & Structures 2013; 36(9): 884–892

41 Maggiolini E, Tovo R, Livieri P. Evaluation of effective stress along the border of lateral notches. Fatigue Fract Engng Mater Struct 39(8), 2016, 1030–1039

42 Lazzarin P, Tovo R. A unified approach to the evaluation of linear elastic stress fields in the neighbourhood of cracks and notches. International Journal of Fracture, 1996, **78**: 3–19

43 Gross R, Mendelson A. Plane elastostatic analysis of V-notched plates. International Journal of Fracture Mechanics, 1972, **8:** 267–276

44 Lazzarin P, Tovo R. A notch stress intensity factor approach to the stress analysis of welds. Fatigue and Fracture of Engineering Materials and Structures, 1998, **21**: 1089–1104

45 Tovo R, Livieri P, 2008. An implicit gradient application to fatigue of complex structures, Eng. Fract. Mech., 75 (7), pp. 1804–1814

46 Peerlings RHJ, de Borst R, Brekelmans WAM, de Vree JHP, 1996. Gradient enhanced damage for quasi-brittle material. International Journal of Numerical Methods in Engineering 39, pp. 3391–3403

47 Livieri P, Salvati E, Tovo R, 2016. A non-linear model for the fatigue assessment of notched components under fatigue loadings International Journal of Fatigue, Vol. 82–3, pp. 624–633

48 Cristofori, A, Livieri, P, Tovo, R, 2009. An application of the Implicit Gradient Method to Welded Structures Under Multiaxial Fatigue Loadings. International Journal of Fatigue, vol. 31, pp. 12–19

49 Capetta, S, Tovo, R, Taylor, D, Livieri, P, 2011. Numerical Evaluation of Fatigue Strength on Mechanical Notched Components under Multiaxial Loadings. International Journal of Fatigue, vol. 33, pp. 661–671

50 Macdonald KA, Haagensen PJ. Fatigue of welded aluminium hollow section profiles, Engineering Failure Analysis 16 (2009) 254–261

51 Tovo R, Livieri P, 2007. An implicit gradient application to fatigue of sharp notches and weldments. Eng. Fract. Mech., 74, pp. 515–526

52 Eurocode No. 3: Design of Steel Structures. Part 1.1: General rules and rules for buildings ENV 1993-1–1: 1992, Brussels

53 Maddox, SJ, 1995. Scale effect in fatigue of fillet welded aluminium alloys. Proc. Sixth International Conference on Aluminium Weldments, Cleveland, Ohio, 77–93

54 Meneghetti, G, 1998. PhD Thesis, University of Padua

55 Ribeiro AS, Gonçalves JP, Oliveira F, Castro PT, Fernandes AA. A comparative study on the fatigue behaviour of aluminium alloy welded and bonded Joints. Proc. Sixth International Conference on Aluminium Weldments, Cleveland, Ohio, 1995:65–76

56 Jacoby, G, 1961. Über das verhalten von schweissverbindungen aus aluminiumlegierungen bei schwingbeanspruchung. Dissertation, Technische Hochschule, Hannover

57 Ohno, H, 1985. Improvement of fatigue strength of alluminium alloy welded joints by toe peening. Welding Institute of Japan Collected Paper Vol. 3. ESDU 91039

58 Person, NL, 1971. Fatigue of aluminium alloy welded joints, *Welding Research Supplement* **50**, 77s-87-s

59 Sidhom N, Laamouri A, Fathallah R, Braham C, Lieurade HP. Fatigue strength improvement of 5083 H11 Al-alloy T-welded joints by shot peening: experimental characterization and predictive approach. International Journal of Fatigue 27 (2005), pp. 729–745

60 Morgenstern C, Sonsino CM, Hobbacher A, Sorbo F. Fatigue design of aluminium welded joints by the local stress concept with the fictitious notch radius of ρ_f=1 mm, International Journal of Fatigue 28 (2006) 881–890

61 Haagensen PJ, Statnikov ES, Lopez-Martinez L. Introductory fatigue tests on welded joints in high strength steel and aluminium improved by various methods including ultrasonic impact treatment (UIT). IIW Doc. XIII-1748–98

62 Brandt D, Lawrence FV, Sonsino, CM, Fatigue crack initiation and growth in ALMG4.5MN butt weldments, Fatigue and Fracture of Engineering Materials and Structures, 24, 2001, 117–126

63 Macdonald KA, Haagensen PJ, Fatigue design of welded aluminum rectangular hollow section joints, Engineering Failure Analysis 6 (1999) 113–130

64 McDowell, KA, "Fatigue behavior of aluminum alloy weldments in a marine environment" (1977). *Retrospective Theses and Dissertations*. 17275

65 Shahani AR, Shakeri I. Experimental evaluation of fatigue behaviour of thin Al5456 welded joints. *Fatigue Fract Eng Mater Struct*. 2019;1–13. https://doi.org/10.1111/ffe.13173

66 Viespoli LM, Leonardi A, Cianetti F, Nyhus B, Alvaro A, Berto F. Low temperature fatigue life properties of aluminum butt weldments by the means of the local strain energy density approach. Mat Design Process Comm. 2019;1:e30. https://doi.org/10.1002/mdp2.30

67 Coughlin R. Fatigue of Aluminum Welds In Canadian Highway Bridges, Master thesis of Applied Science, Waterloo, Ontario, Canada, 2010

68 James MN, Lambrecht HO, Paterson AE. Fatigue strength of welded cover plates on 6261 aluminium alloy Ibeams, *Int J Fatigue* 15 No 6 (1993) pp. 519–524

69 Tveiten BW, Wang X, Berge S. Fatigue assessment of aluminum ship details by hot-spot, stress approach, ABS technical papers, 2007, pp. 255–271

70 Hirt, MA, Smith, IFC. Fatigue behaviour of aluminium beams with welded attachments. Proceedings, 5th INALCO Conference on Aluminium Weldments, Munich, 27–29 April 1992